# Repeatability of adaptation in sunflowers: genomic regions harbouring inversions also drive adaptation in species lacking an inversion

Shaghayegh Soudi[1+], Mojtaba Jahani[1,2+], Marco Todesco[2,3,4], Gregory L. Owens[5], Natalia Bercovich[2], Loren H. Rieseberg[2], Sam Yeaman[1,*]

+Joint first-authors

Author affiliations:

1. Department of Biological Sciences, University of Calgary, 2500 University Drive NW, Calgary, Canada, T2N 1N4
2. Department of Botany, University of British Columbia, 6270 University Blvd, Vancouver, Canada, V6T 1Z4
3. Michael Smith Laboratories, University of British Columbia, 6270 University Blvd, Vancouver, Canada, V6T 1Z4
4. Irving K. Barber Faculty of Science, University of British Columbia Okanagan, 3187 University Way, Kelowna, Canada, V1V 1V7
5. Department of Biology, University of Victoria, 3800 Finnerty Rd, Victoria, Canada, V8P 5C2

*corresponding author: Sam Yeaman, samuel.yeaman@ucalgary.ca

**Abstract**

Local adaptation commonly involves alleles of large effect, which experience fitness advantages when in positive linkage disequilibrium (LD). Because segregating inversions suppress recombination and facilitate the maintenance of LD between locally adapted loci, they are also commonly found to be associated with adaptive divergence. However, it is unclear what fraction of an adaptive response can be attributed to inversions and alleles of large effect, and whether the loci within an inversion could still drive adaptation in the absence of its recombination-suppressing effect. Here, we use genome-wide association studies to explore patterns of local adaptation in three species of sunflower: *Helianthus annuus*, *H. argophyllus*, and *H. petiolaris*, which each harbour a large number of species-specific inversions. We find evidence of significant genome-wide repeatability in signatures of association to phenotypes and environments, which are particularly enriched within regions of the genome harbouring an inversion in one species. This shows that while inversions may facilitate local adaptation, at least some of the loci can still harbour mutations that make substantial contributions without the benefit of recombination suppression in species lacking a segregating inversion. While a large number of genomic regions show evidence of repeated adaptation, most of the strongest signatures of association still tend to be species-specific, indicating substantial genotypic redundancy for local adaptation in these species.

## Introduction

The genetic basis of local adaptation is sometimes highly repeatable, with examples of large effect genes driving responses in multiple species, such as *FT* affecting flowering time in numerous plants (Izawa 2007; Auge et al. 2019) or *Mc1r* driving colour polymorphisms in vertebrates (Manceau et al. 2010; Rosenblum et al. 2014). Local adaptation can also be repeated for polygenic traits, with significant patterns of similar association found across many loci for comparisons of conifers (Yeaman et al. 2016), maize and its wild relative teosinte (Tittes et al. 2021; Wang et al. 2021), and *Brassicaceae* (Bohutínská et al. 2021), to name a few. While we have a growing number of examples of repeatability in the basis of adaptation, it is also interesting to know if species use different genes to adapt to the same selection pressure. Genotypic redundancy – the potential for many genotypes to yield a given phenotype – is one critical factor affecting the repeatability of adaptation, as high redundancy would be expected to

result in lower repeatability (Yeaman et al. 2018). Another critical factor affecting repeatability is shared standing variation, whether present due to introgression or incomplete lineage sorting. In either case, variants shared among lineages are much more likely to contribute to a repeated response than new mutations (MacPherson and Nuismer 2018; Ralph and Coop 2015). Consistent with this, Bohutínská and colleagues (2021) found that repeatability was negatively related to phylogenetic distance. While we are now accumulating more studies about the repeatability of adaptation, we still have very few examples and much remains unknown about the relative importance of these factors (Yeaman 2022).

Inversions have been implicated in local adaptation in many species (Wellenreuther and Bernatchez 2018), likely due to their effect to suppress recombination among inverted and non-inverted haplotypes, and thereby maintain LD among beneficial combinations of locally adapted alleles (Rieseberg 2001; Noor et al. 2001; Kirkpatrick and Barton 2006). This has been approached by models studying the establishment of inversions that capture combinations of locally adapted alleles present as standing variation (*e.g.*, Kirkpatrick and Barton 2006), as well as models examining the accumulation of locally adapted mutations within inversions (*e.g.*, Schaal et al. 2022). If there is variation in the density of loci that can potentially contribute to local adaptation, inversions would be expected to preferentially establish and be retained in regions harbouring a high density of such loci (and this expectation would hold for both the capture and accumulation models). We would also expect to see stronger signatures of repeated local adaptation in such high density regions. Despite mounting evidence of their importance in adaptation, it is unclear how inversions may covary with repeatability of adaptation among species. A fundamental parameter of importance in these models is the relationship between migration rate and strength of selection on individual alleles, which may not make persistent contributions to local adaptation without the suppressing effects of recombination if selection is too weak (Yeaman and Whitlock 2011; Bürger and Akerman 2011). If most alleles have small effects relative to migration rate and can only contribute to local adaptation via the benefit of the recombination-suppressing effect of an inversion, then we would expect little repeatability at the site of an inversion – other species lacking the inversion would not tend to use that same region for adaptation because selection would be too weak for alleles to persist. On the other hand, if some loci are particularly important for local adaptation and regularly yield mutations of large

effect, with these patterns being conserved among species, repeatability within regions harbouring inversions may be substantial. Thus, studying whether adaptation at the same genomic region harbouring an inversion is observed in other species lacking the inversion can give insights about the underlying architecture of adaptation, and the evolution and maintenance of inversions.

Here, we explore the repeatability of local adaptation in three species of sunflowers, *Helianthus annuus*, *Helianthus argophyllus* and *Helianthus petiolaris* (Figure 1), which harbour large regions of suppressed recombination ("haploblocks"), most of which are inversions, and are often associated with adaptive traits (Todesco et al. 2020). *Helianthus annuus*, the common sunflower, is the closest wild relative of cultivated sunflower, which was domesticated from it around 4,000 years ago (Blackman et al. 2011). Populations of *H. annuus* are distributed throughout the central and western USA and generally found on mesic soils, but can grow in a variety of disturbed or extreme habitats, such as semi-desertic or frequently flooded areas, as well as salt marshes. *Helianthus petiolaris*, the prairie sunflower, prefers sandier soils, and ecotypes of this species are adapted to sand sheets and sand dunes (Ostevik et al. 2016). Here we include samples from two subspecies: *H. petiolaris ssp. petiolaris*, which is commonly found in the southern Great Plains, and *H. petiolaris ssp. fallax*, which is limited to more arid regions in Colorado, Utah, New Mexico and Arizona (Heiser et al. 1969). *Helianthus petiolaris* and *H. annuus* have broad and overlapping distributions throughout the central and western United States and appear to have adapted to similar changes in temperature, moisture and photoperiod regimes. There is also evidence indicating *H. annuus* and *H. petiolaris* have likely been exchanging genes during much of their history of divergence (Strasburg and Rieseberg 2008), although partially isolated by strong pre- and post-zygotic barriers (Sambatti et al. 2012). The third species, *Helianthus argophyllus*, the silverleaf sunflower, is found exclusively in the southeast coast of Texas and includes both an early flowering ecotype on the coastal barrier islands and a late flowering ecotype inland (Moyers and Rieseberg 2016; Todesco et al. 2020). *H. argophyllus* is thought to have undergone cycles of sympatry and allopatry with *H. annuus* and *H. petiolaris* over time, but currently only overlaps with *H. annuus,* with thus overlap likely being a recent event (Heiser, 1951).

Using broad sampling across the ranges of these species (Figure 1) and sequencing data first published by Todesco et al. (2020), we study the genomic basis of local adaptation by conducting genome-wide scans for associations with climatic and soil environmental variables and phenotypes measured in a common garden. An inherent problem in studying the basis of local adaptation is accounting for the covariance between genome-wide population genetic structure and environment. When the selection pressure driving local adaptation tends to parallel a main axis of demographic expansion or isolation by distance, neutral alleles will have spatial patterns resembling those of causal alleles. Methods that do not correct for population structure have large numbers of false positives because allele frequencies at neutral loci tend to correlate with the environment more than expected by chance (Lotterhos and Whitlock 2014). By contrast, methods that use structure correction tend to suffer from false negatives because the causal loci have similar patterns of allele frequency variation as the genomic background, and so their statistical signatures are decreased (DeRaad et al. 2021; Booker et al. 2023b). When a non-corrected approach is applied to multiple species, the false positive problem can be mitigated when testing for loci that contribute to repeated adaptation, as the same gene should not tend to be a false positive in multiple species more often than expected by chance (Yeaman et al. 2016). Here we use a conventional GWAS approach with structure correction to study the basis of phenotypes, which vary both within and among populations, and use an uncorrected approach to test association to environment, which only varies among populations (as all individuals within the same population have the same value of environmental variable). For the environmental association portions of the study, we also explore the effect of structure correction in some analyses, to contrast the false negative vs. false positive problem inherent in each approach. We apply these approaches individually to *H. annuus*, *H. argophyllus*, and the two *H. petiolaris* subspecies, and make pairwise and higher-order comparisons among combinations of these four lineages to study repeatability.

Our overall aim is to characterize the extent of repeatability of local adaptation for different traits and environments, and explore the importance of inversions and other factors that may drive differences in repeatability. This analysis builds upon the work of Todesco et al. (2020), which focused on the evolution of haplobocks within each species, but did not systematically study patterns of repeatability in signatures of association among species. We begin by using the

148 strength of correlations between environment and phenotypes measured in a common garden to
149 identify which environmental variables are likely driving local adaptation within each species,
150 and use an index to quantify the relative similarity in these patterns among pairs of species (see
151 Figure S1 for a schematic overview of methods and research questions). We then conduct
152 Genome-Wide Association tests to identify regions most strongly associated with phenotypes
153 and environments within each species. To assess the similarity in these association statistics
154 among species, we use methods similar to Yeaman et al. (2016) to identify regions of the
155 genome that exhibit greater similarity in signatures of association among pairs of lineages than
156 expected by chance, which are likely driven by repeated adaptation using the same genes (but not
157 necessarily the same alleles). We then explore how the number and total size of these regions of
158 repeated association covary with the index of similarity in environmental importance. We also
159 explore whether these regions of repeated association tend to covary with patterns of shared
160 standing variation and test if they are enriched within previously identified haploblocks, to
161 explore the role of inversions in adaptation. We then identify candidate genes that show
162 particularly strong signatures of repeated association across multiple lineages. Finally, based on
163 the number of signatures of association that are shared vs. non-shared among lineages, we
164 estimate the number of regions genome-wide that could potentially contribute to local adaptation
165 for each variable and phenotype, which is related to the genotypic redundancy. Taken together,
166 our results show that local adaptation in sunflowers tends to involve both strong repeatability at a
167 small number of genes, often associated with inversions, coupled with high redundancy and non-
168 repeated responses across a much larger number of loci.
169
170
171
172

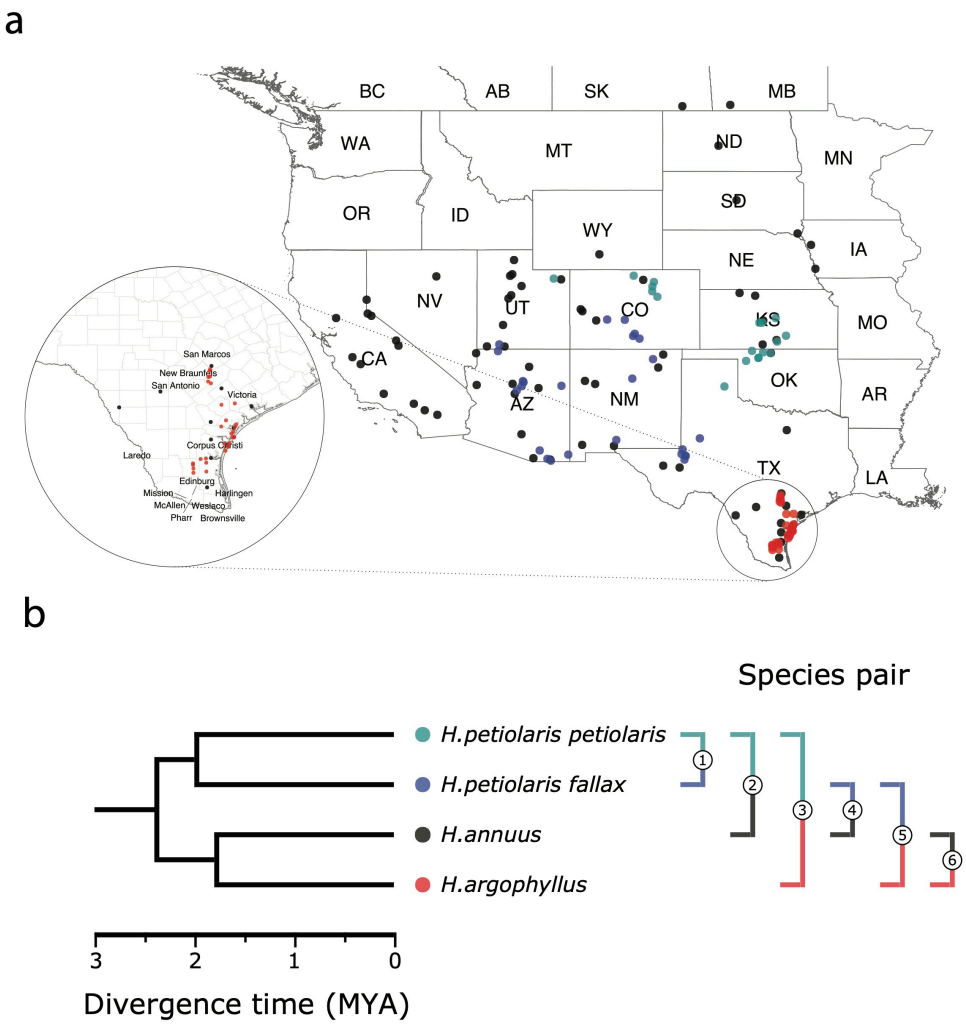


**Figure 1.** Sampling sites and phylogenetic relationship among surveyed species. (a) Sampling locations of wild sunflower populations studied in the present study, and (b) phylogenetic relationship of the four (sub-)species. Numbered brackets represent the six pairwise comparisons performed in this study.

## Results

**Local adaptation at the phenotypic level.** The four taxa vary considerably in the breadth of environmental variation spanned by their respective ranges, with *H. annuus* spanning the widest niche and *H. argophyllus* spanning the narrowest (Figure 2A). Using the correlation between phenotype and environment as a metric of the strength of local adaptation on individual traits, we

observe strong correlations for many combinations (Figure S2), suggesting that local adaptation is quite pronounced for some traits. To quantify the similarity among pairs of species in the strength of local adaptation at the phenotypic level (and to later compare this to results at the genomic level), we calculate an index we refer to as the Similarity in Phenotype-Environment Correlation (SIPEC), which is maximized when both species have strong correlations (in either direction) between a phenotype and environmental variable (see Methods). For each environmental variable, we take the maximum value of SIPEC across all phenotypes as a relative measure of the importance of the variable for driving local adaptation in both species (such that when SIPEC is low, the variable is not a strong driver of phenotypic adapatation in at least one of the two species). We find the largest values of SIPEC for temperature variables and the smallest values for soil types, and generally find higher values for comparisons between the *petiolaris* subspecies (Figure S3).

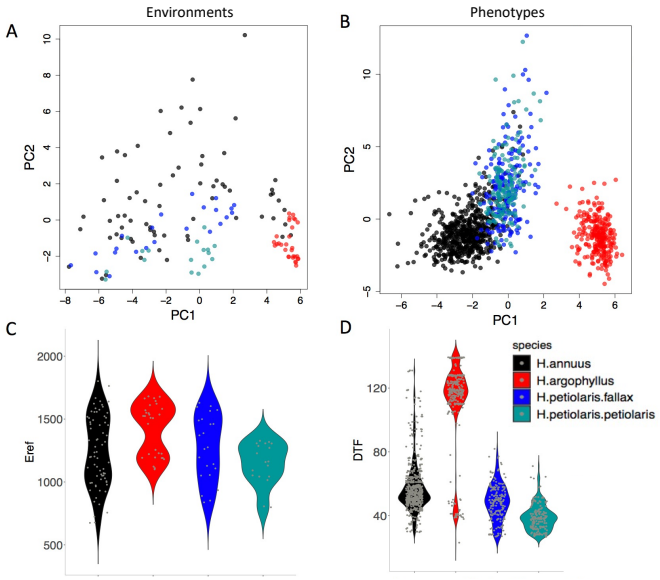


**Figure 2.** The range of environmental and phenotypic variation in the studied species. Variation in environment (a) and phenotype (b) for the studied species, along the two largest axes of a Principle component analysis (PCA). Violin plots show two examples of variation in environment (Hargreaves reference evapotranspiration index; Eref) and phenotype (Days to Flower; DTF) within and among the taxa (c,d).

208

209 **Genome-wide analysis of repeated local adaptation.** To search for regions of the genome
210 driving repeated adaptation in multiple taxa, we first identified windows of the genome within
211 each species that showed strong signatures of association to either phenotype (GWAS; with
212 structure correaction) or environment (GEA; without structure correction), referred to as "top
213 candidate" windows. To identify Windows of Repeated Association (WRAs) between pairs of
214 species, we then assessed whether top candidate windows identified in one focal taxon also
215 tended to be enriched for strong signatures of association to the same environment or phenotype
216 in each of the other taxa (using the null-W test, which tends to be more sensitive than just finding
217 the overlap between the top candidate windows; See Methods). As recombination rate can affect
218 the sensitivity of these kinds of window-based genome scans (Booker et al. 2020), the
219 identification of WRAs was conducted after binning windows by recombination rate, although in
220 many cases we did not observe substantial differences in the null distributions among these bins
221 (*e.g.*, Figure S4). This analysis revealed many windows with signatures of repeated association,
222 with the strongest repeated signature found for Number of Frost-Free Days (NFFD; Figure 3A;
223 S4), but also showed that many of the windows with the strongest association in one species did
224 not have strong signatures in other species (Figure 3B).

225 Under the null hypothesis that all regions of the genome evolve neutrally due to drift and
226 independently in each species, ~5% of the top candidate windows identified in one species
227 would be expected to fall into the tail of the null distribution of another species (*i.e.*, be classified
228 as WRAs). While we find significantly more WRAs than the 5% expected by chance, ranging
229 from 6.3% to 44.1% (mean = 14.5%; Figure S5), multiple factors can violate the assumptions of
230 this test and increase the proportion of windows classified as WRAs. Most importantly,
231 similarity in signatures of association can be driven by shared ancestral variation or ongoing
232 introgression, and this must always be considered as an alternative explanation. It is clear that
233 most regions of the genome harbour some shared standing variation between all 6 pairwise
234 comparisons of the taxa, whether due to segregating ancestral variation or introgression, based
235 on an index quantifying the proportion of shared to non-shared SNPs in each window (Figure
236 S6). However, we do not find consistent differences in the amount of shared standing variation
237 within windows when comparing WRAs with the rest of the genome (Figure S6). Thus, while

238 introgression may make subtle contributions to WRAs, a lack of increased shared standing
239 variation in the significant windows suggests that it is not a primary driver of these patterns.
240

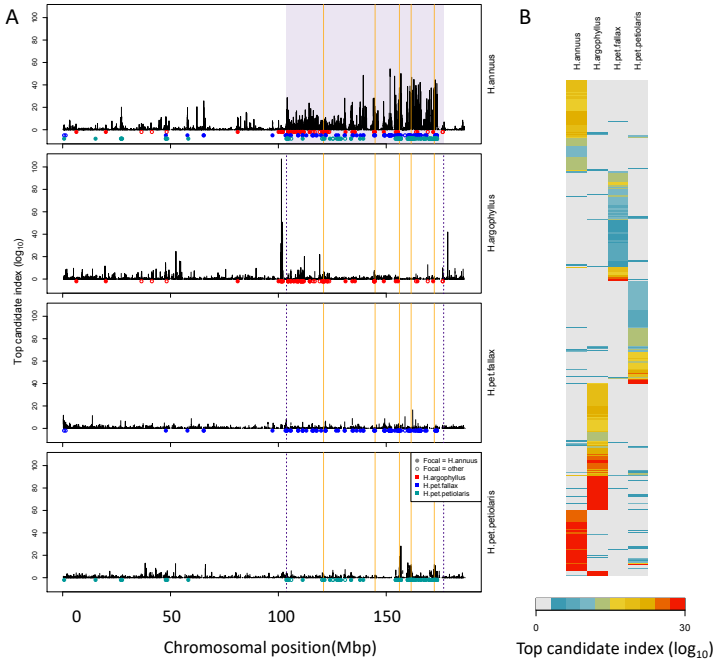


241

242 **Figure 3**. Signatures of association for Number of Frost-Free Days (NFFD) in the four taxa on
243 chromosome 15 (A) and genome-wide (B). Panel A shows Windows of Repeated Association
244 (WRAs; coloured bars) for comparisons between the focal species, *H. annuus*, and each of the
245 other 3 taxa, with the haploblocks in *H. annuus* shaded in violet and the regions with significant
246 PicMin hits as vertical orange lines. Panel B shows the value of the top candidate index for each
247 of the 1000 windows with the strongest signatures of association in at least one species (~top 2%
248 of genome-wide windows). Rows are ordered using hierarchical clustering to group windows
249 with similar patterns across multiple species, illustrating the extent of overlap/non-overlap in the
250 windows with strongest signatures in each species (*i.e.*, position in the figure does not reflect
251 chromosomal position).
252
253

254 A second source of inflation in the number of WRAs is due to hitchhiking: if a given
255 locus is a true positive driving adaptation, LD with other windows in tight physical linkage will
256 result in spurious correlations causing them to also be classified as WRAs increasing the
257 genome-wide proportion above 5%, and this effect will be particularly exaggerated in
258 haploblocks. To control for this, we binned neighbouring WRAs together that exhibited high LD
259 (>95$^{th}$ percentile) over short spans of the genome (<1 cM) in either species, yielding regions we
260 refer to as Clusters of Repeated Association (CRAs). While this clustering method should

261 provide a partial control for the effect of hitchhiking, we note that the number of CRAs cannot be
262 taken as a reliable estimate of the number of independent targets of natural selection. Instead, we
263 treat the number and size of these CRAs as proxies for the relative genome-wide similarity in
264 association between each pair of species, and conduct downstream analyses to test hypotheses
265 about the factors driving local adaptation.
266 CRAs varied in number and size across the 6 pairwise-species comparisons, with
267 particularly large CRAs identified at the sites of known haploblocks (Todesco et al. 2020). For
268 CRAs identified for phenotypic associations, their extent ranged from 168 clusters spanning
269 48,524,903 bp (covering only 1.6% of the genome) in *H.argophyllus-H.pet.petiolaris* to a
270 maximum of 1,667 clusters spanning 426,409,647 bp (14.2 % of the genome) in *H. pet.*
271 *petiolaris-H. pet. fallax* (Figure S7). CRAs identified for environmental variables tended to be
272 more numerous and cover a larger region of the genome, varying from 1154 clusters comprising
273 15% of the total genome for *H. argophyllus-H. pet. fallax* up to 2,260 distinct clusters covering
274 29% of the genome between *H. petiolaris* subspecies (Figure S8). The large extent of the
275 genome covered by CRAs is mainly driven by their occurrence within many different
276 haploblocks, which tend to be unique to each species and cover substantial portions of their
277 genomes (Todesco et al. 2020). Genes within CRAs tend to be enriched for a large number of
278 GO terms spanning many different categories (Figure S9, S10). When we use an approach that
279 corrects for population structure in the genotype-environment association tests (Baypass), we
280 find substantially reduced numbers of CRAs (Figure S11). This reduction is likely due to
281 reduced power to detect true positive causal loci when population structure covaries with
282 environment, as true positives do not "stand out" relative to the genomic background (Booker et
283 al. 2023b). While single-species association tests without correction for population structure
284 typically yield large numbers of false positives, the null-W test comparing association results
285 across species accounts for the chance that the same region is a false positive in both species
286 (Yeaman et al. 2016).
287
288
289 **Repeated association in the genome reflects patterns at the phenotypic level.** If natural
290 selection is driving repeated patterns of local adaptation in the genomes of two species, we
291 should see greater similarity for associations with environmental variables that are also strongly

292 associated with phenotypic variation in both species. Consistent with this prediction, we found
293 that environmental variables with a high maximum SIPEC index (*i.e.*, high correlation between
294 environment and some axis of phenotypic variation in both species; Figure S3) also tended to
295 have a larger number of CRAs (Figure 4), with higher repeatability at both the phenotype and
296 genome level for temperature-related variables and much lower repeatability for soil-related
297 variables (with similar patterns for mean SIPEC index; Figure S12). Unfortunately, given the
298 non-independence of environmental variables there is pseudo-replication in these data so it is not
299 possible to conduct a formal significance test of these patterns. In all cases, the number of CRAs
300 exhibited a weak negative relationship with the index of standing variation, with environmental
301 variables that had the greatest number of CRAs having the lowest relative amounts of shared
302 standing variation (Figure S13). This suggests that the observed similarity in patterns of
303 association among species is not being strongly driven by incomplete lineage sorting or
304 introgression, as we would expect a positive relationship between the index of shared standing
305 variation and the number of CRAs. We found similar but weaker patterns in the association
306 between SIPEC and size of CRAs (Figure S14). The weakening of these patterns relative to those
307 for number of CRAs may reflect comparatively greater contribution of haploblocks driving
308 patterns with size rather than number (*i.e.*, if a particularly large haploblock is a CRA, then that
309 variable will have a particularly large value relative to its actual importance for local adaptation).

310

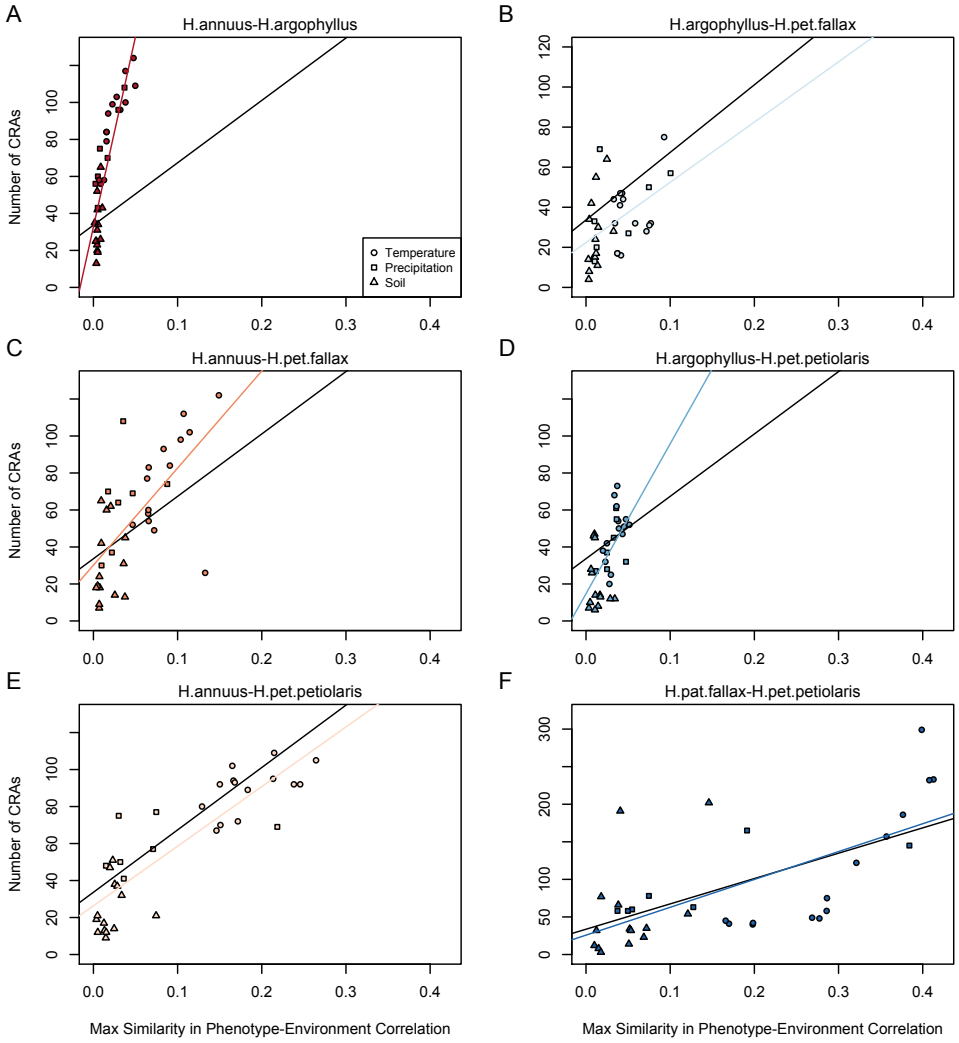


**Figure 4.** Relationship between maximum Similarity in Phenotype-Environment Correlation (SIPEC) and number of Clusters of Repeated Association (CRAs). SIPEC was calculated for each phenotypic PCA axis with the maximum taken across the axes that cumulatively explain 95% of the phenotypic variance, for each environment. Each panel includes both a linear model fit to the data within the panel (coloured lines), and a linear model fit to all data simultaneously (black lines) for comparison. Note that because environmental variables are correlated, these points are not independent and therefore represent a source of pseudoreplication, preventing formal statistical tests of this relationship.

**Overlap of signatures of repeated association with low recombination haploblocks.**

Inversions can facilitate local adaptation by suppressing recombination between locally adapted alleles within the inverted vs. ancestral haplotypes (Kirkpatrick and Barton 2006). If a given

326 species exhibits a signature of association to environment at a segregating inversion, it is
327 interesting to test whether similar signatures of association are found in other species that lack a
328 segregating inversion at the same region of the genome. This would suggest that particularly
329 strong selection is acting on loci in this region, as signatures of association can still evolve even
330 without the recombination suppressing effect of the inversion. While not all of the low-
331 recombination haploblocks identified by Todesco et al. (2020) have been validated as inversions,
332 for simplicity we treat each haploblock as representative of a segregating inversion. The majority
333 of these haploblocks are present as segregating variation in only one of the three species, but
334 when they occur in *H. petiolaris*, they tend to be found as segregating variation within both
335 subspecies. Thus, if we find significant enrichment of the regions of repeated association (WRAs
336 and CRAs) within haploblocks, this suggests that both the species with a segregating inversion
337 and the species lacking an inversion are using this region of the genome to drive local adaptation.
338 As a first test of this relationship, we assessed two-way contingency tables for whether top
339 candidate windows within a species were also significant windows of repeated association
340 (WRA/non-WRA) and whether they fell within haploblocks (yes/no). This approach controls for
341 the potential enrichment of top candidate windows within haploblocks relative to the rest of the
342 genome and asks if the proportion of WRAs within haploblocks is even higher than non-WRA
343 top candidate windows. For most phenotypes and environments, we found that the proportion of
344 WRAs occurring within haploblocks was much higher than the proportion of non-WRAs
345 occurring within haploblocks (Figure 5). Across all species comparisons and
346 environmental/phenotypic variables, a total of 310 contrasts showed significant enrichment for
347 WRAs in haploblocks, compared to only 23 contrasts showing a significantly higher proportion
348 of non-WRAs in haploblocks (note that because of non-independence of the phenotypes and
349 environmental variables, there is pseudo-replication inherent in these estimates). In *H.*
350 *argophyllus*, while non-WRA top candidates tended to fall within haploblocks less commonly
351 than in the other taxa, WRAs tended to be very strongly enriched within haploblocks (Figure
352 5B). As a follow-up, we also tested whether CRAs were enriched within haploblocks (without
353 controlling for whether top candidate windows also tended to be enriched), also finding strongly
354 significant enrichment of CRAs within haploblocks for many traits and environments (Figure
355 S7C & D). Broad patterns revealed by these analyses are similar, as both show that genomic
356 regions harbouring haploblocks tend to be enriched for signatures of association to environment

in species lacking the haploblock. It is noteworthy that few significant signatures of enrichment in haploblocks were found for *H. petiolaris petiolaris* vs. *H. petiolaris fallax* (Figure S7C & D), perhaps because extensive introgression across non-locally adapted regions of the genome obscures true signal.

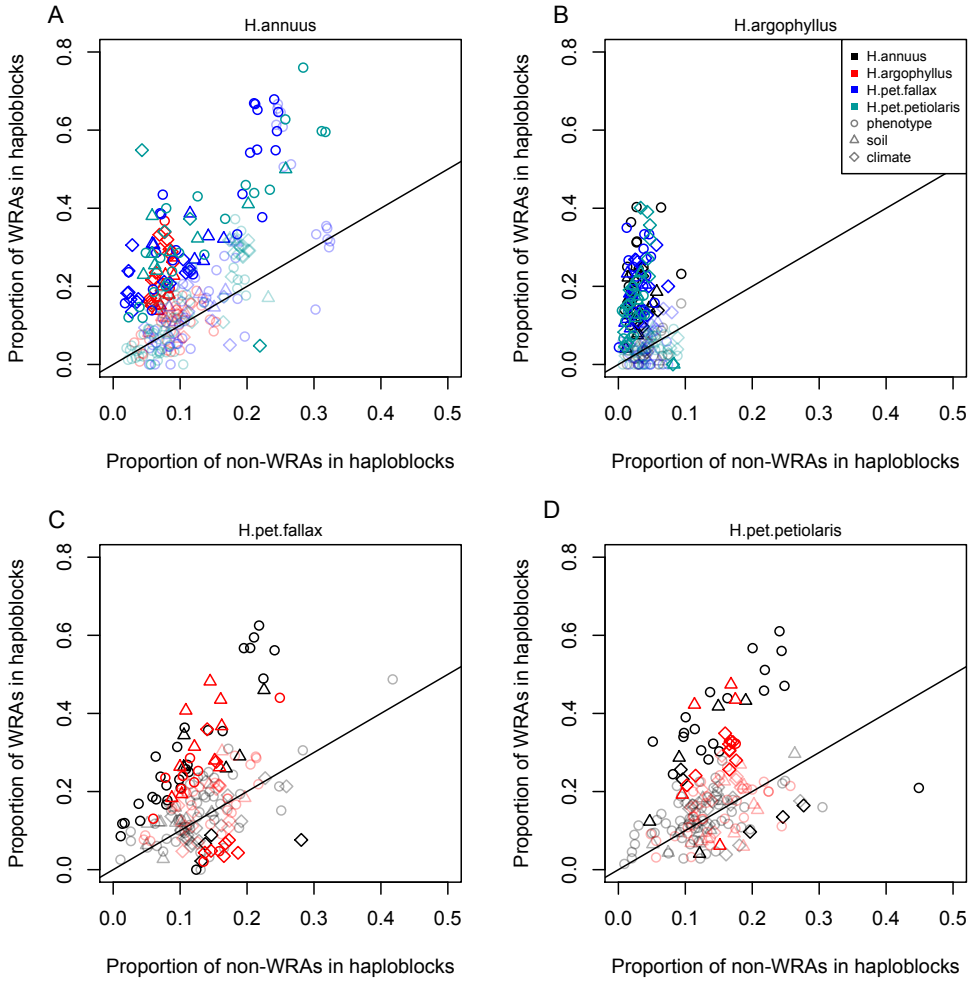


**Figure 5.** Enrichment of signatures of repeated association within genomic regions harbouring a haploblock in one of the two compared lineages. Each panel shows the proportion of top candidate windows that fall within haploblocks for windows with significant signatures of repeated association by the null-W test (WRAs) vs. those with non-significant signatures (non-WRAs). Comparisons of *H. petiolaris petiolaris* vs. *H. petiolaris fallax* are omitted as they share segregating haploblocks. Each point corresponds to the results for a single phenotype or environment, with dark shading used for cases where the deviation from random for the contingency table is significant by a permutation test ($p < 0.05$), and lighter shading indicating a non-significant result. Note that because many environmental variables and phenotypes are correlated with each-other, these points are not independent and therefore represent a source of pseudoreplication, preventing formal statistical tests of the overall relationship within each panel.

375

376 **Multi-species signatures of repeated association.** As a complement to the pair-wise analyses
377 described above, we also conducted an analysis using PicMin, which simultaneously considers
378 any number of lineages to identify genes with particularly strong and repeated signatures of
379 association (Booker et al. 2023a). After identifying significant windows clustering together those
380 < 1 Mbp apart, we found a total of 145 regions that were significant for at least one
381 environmental variable or phenotype (at FDR < 0.1 applied within each variable). The largest
382 number of significant regions for environment was found with the Number of Frost-Free Days
383 variable (20 with FDR < 0.1; 44 with FDR < 0.2) and for phenotypes with Total Leaf Number, a
384 measure of developmental timing of flowering (9 with FDR < 0.1; 19 with FDR < 0.2).
385 Considering the 720 individual 5000 bp windows with FDR < 0.2 for at least one variable, 387
386 (53.8%) are within 500 bp of a genic region, representing a 2.3x enrichment relative to the rate
387 for windows that were not significant hits using PicMin (23.3% of other windows fall within 500
388 bp of a genic region; $X^2$ test $p < 10^{-15}$).
389

390

391 **Estimating the number of potentially adaptive loci.** Even for the environment with the highest
392 repeatability (Number of Frost-Free Days; NFFD), most of the strongest signals of association
393 are found in only one lineage (Figure 3B). Unfortunately, while the null-W test provides strong
394 support and controls false positives when identifying repeated association, regions of the genome
395 with strong associations in only a single species may include a large (and unknown) number of
396 false positives. Thus, while it is biologically interesting to know how much adaptation is non-
397 repeated among species, it is difficult to quantify with certainty (Booker et al. 2023a; Booker et
398 al. 2023b). Under the assumption that at least some of the non-repeated signatures of association
399 are true positives, this implies that there is considerable genotypic redundancy, with many
400 different ways for these species to adaptively respond to variation in the same environment. To
401 estimate the number of windows that could potentially contribute to local adaptation for each
402 variable ($L_{eff}$), we modified the method of Yeaman et al. (2018) to partially account for the effect
403 of linkage among nearby windows (see methods). This method assumes that the windows with
404 signatures of association in each species are a random draw from a larger number of potentially

contributing windows ($L_{eff}$), which can be inferred based on the ratio of shared vs. non-shared windows with strong association signatures (see Methods). We find that estimates of $L_{eff}$ tend to be large, always well over 1000 windows regardless of the trait or environment (Figure S15A). There are numerous sources of error that affect the estimation of $L_{eff}$, which will tend to be overestimated due to linkage (Figure S15A) or when many signatures of association are false positives (see supplementary results), and will be underestimated when some repeatability is due to shared standing variation (Yeaman et al. 2018). Even after controls for linkage and assuming a high false positive rate of 80%, estimates of $L_{eff}$ remain in the hundreds even for the variable with the lowest value of $L_{eff}$ (Eref; Figure S15C, D).

## Discussion

Despite its critical importance in shaping the architecture of adaptation, little is known about the extent of genotypic redundancy underlying different traits (Barghi et al. 2020; Láruson et al. 2020; Yeaman 2022). Here, we have shown evidence of significant repeatability in the basis of local adaptation (Figure 4, 5), but also an abundance of species-specific, non-repeated signatures (Figure 3; S14). In particular, we find that regions of the genome that harbour inversions in one species also tend to be strongly enriched for signatures of association in other species lacking the inversion (Figure 5). Taken together, this suggests that local adaptation in these species is highly flexible – different species apparently use quite different sets of loci to adapt to the same environment – yet still involves some component that has minimal redundancy, with inversions playing a particularly important role. Some of the "usual suspects" show up in the set of significantly repeated loci identified by PicMin: in addition to the homologs of the *FT* (*FLOWERING LOCUS T*) gene reported by (Todesco et al. 2020), we also found hits for several other genes involved in circadian regulation and flowering time, including *PRR3* (Para et al. 2007), *TOE1* (Aukerman and Sakai 2003), and *PHYC* (Takano et al. 2005; Chen et al. 2014), which is known to regulate photoperiodic responses in Arabidopsis accessions (Balasubramanian et al. 2006). Other top hits included genes involved in plant development and auxin transport (*PIN3*; (Keuskamp et al. 2010), *ARF4* (Pekker et al. 2005), and *MN*; (Bhatia et al. 2016)), and plant immunity (*CRK13* (Acharya et al. 2007) and *PRR2* (Cheval et al. 2017))

435 The increased repeatability found in regions of the genome that harbour inversions in only
436 one species is particularly interesting. Inversions are commonly associated with local adaptation
437 (Wellenreuther and Bernatchez 2018), likely because they reduce the rate at which
438 recombination breaks up combinations of co-selected alleles (Kirkpatrick and Barton 2006),
439 which perhaps facilitates contributions by alleles that would be individually too weakly selected
440 to overcome swamping by migration (Bürger and Akerman 2011; Yeaman and Whitlock 2011;
441 Schaal et al. 2022). Evidence here suggests these regions still tend to contribute to adaptation in
442 the species lacking the recombination-suppressing effect of an inversion, consistent with a strong
443 effect of selection relative to migration on at least one locus in the region (rather than adaptation
444 exclusively via many alleles of small effect; Yeaman 2022). As an example, chromosome 15
445 harbours a large (72 Mbp) haploblock in *H. annuus* that is strongly associated with NFFD
446 (Number of Frost-Free Days), and also shows some signatures of association in the other taxa,
447 with particularly strong signatures of association on either side of the haploblock in *H.*
448 *argophyllus* (Figure 3A). Interestingly, loci of repeated association identified by PicMin within
449 this region include two genes whose homologs are known to regulate responses to cold: *COLD-*
450 *RESPONSIVE PROTEIN KINASE 1*,*CRPK1* (Liu et al. 2017) and *LATE ELONGATED*
451 *HYPOCOTYL*, *LHY* (Mizoguchi et al. 2002; Dong et al. 2011). It seems likely that strong
452 selection relative to migration is therefore acting upon several loci in this region, and in many
453 others harbouring inversions.
454 The observed repeatability associated with inversions further supports the local adaptation
455 model as an explanation for the long-term persistence of segregating inversions (at least in
456 sunflower), rather than mechanisms based on dominance or meiotic drive (Rieseberg 2001). If
457 there is variation across the genome in the density of loci with the potential to be involved in
458 local adaptation, then the establishment and maintenance of inversions would be biased towards
459 regions harbouring a high density such loci under this model. If the genomic basis for local
460 adaptation is conserved amongst species, then these same regions are more likely to have high
461 repeatability. Thus, our observation of genomic regions harbouring inversions also being
462 enriched for WRAs is consistent with this general model for inversion evolution. Unfortunately,
463 our observations do not provide much insight into whether inversions evolve through the capture
464 (*e.g.* Kirkpatrick and Barton 2006) or accumulation (*e.g.* Schaal et al. 2022) type of model, as
465 either model would be consistent with our results. Most of the the sunflower inversions are >1

466 My old, and therefore predate any current local adaptation patterns, but likely do not predate the
467 genes underlying local adaptation (which appear to be shared among the species we studied). As
468 for the alleles underlying local adaptation, they may be younger than the inversions, but as our
469 work suggests, these regions are prone to harbouring locally adaptive alleles so it is possible that
470 they also harboured other ancestral locally adaptive alleles. While many studies have
471 demonstrated the importance of inversions for adaptation (Wellenreuther and Bernatchez 2018;
472 Hager et al. 2022), to our knowledge only two other studies have documented the involvement of
473 the same loci making contributions in the absence of the recombination-suppressing effect of the
474 inversion (Lee et al. 2017; Coughlan and Willis 2018). This also highlights how comparative
475 studies of a species lacking an inversion may help identify which genes are driving adaptation in
476 another species with an inversion, as segregating inversions tend to have extensive LD that
477 prevents identification of any potential targets of natural selection within them.

478 While our results suggest a large number of loci can potentially contribute to adaptation,
479 implying high redundancy (Figure 3B; S14), there are several factors that complicate inference.
480 Separating the effects of drift and selection to detect signatures of local adaptation is notoriously
481 difficult, because population structure often covaries with features of the environment that drive
482 adaptation (Lotterhos and Whitlock 2014; Hoban et al. 2016; DeRaad et al. 2021). As found by
483 other analyses (Yeaman et al. 2016; DeRaad et al. 2021), when we use structure correction in our
484 genotype-environment association tests, we find many fewer signatures of repeated association
485 (Figure S7 vs. S11), likely due to the reduced power of Baypass to detect true positives when the
486 environment covaries with population structure (Booker et al. 2023b). Here, we have side-
487 stepped the issues involved in correction for population structure by instead relying on
488 comparisons among species to identify loci with associations more extreme than expected by
489 chance in multiple species, using the null-W and PicMin tests. This assumes that most loci in the
490 genome are not involved in local adaptation, so that the relatively small proportion that are
491 driving adaptation can therefore be picked out due to their tendency to fall into the tail of the
492 distribution of association statistics in at least one other species (which would only occur at the
493 rate of random chance under a purely neutral model). While this approach should be relatively
494 robust for identifying loci with repeated patterns of adaptation, there is no way to formally
495 estimate significance of associations found in only a single species, many of which may be false

496 positives due to covariation of population structure and environment. However, even if we
497 assume that 80% of the observed non-repeated loci are false positives, we still find that estimates
498 of the effective number of loci contributing to adaptation ($L_{eff}$) are in the hundreds (Figure
499 S15C). As we are unable to detect loci of small effect due to the limited power, but these loci
500 still likely make important contributions to heritability, our estimates of $L_{eff}$ will also be biased
501 downwards by excluding these potentially important drivers. Finally, it is also difficult to
502 exclude the contribution of introgression or incomplete lineage sorting to the observed signatures
503 of repeated association. If a locus tended to be highly introgressed between two species in a
504 restricted region of their range, it is possible it could also covary with environment and therefore
505 result in a signature of repeated association that would be mistakenly interpreted as adaptation.
506 While it is difficult to preclude this from our analysis, regions of the genome with signatures of
507 repeated association do not tend to have higher levels of shared standing variation than
508 background regions (Figure S6), suggesting this is not a broad explanation for our observations.
509 If anything, shared standing variation would be expected to increase repeatability of adaptation
510 (MacPherson and Nuismer 2017), adding further weight to the inference that there is high
511 genotypic redundancy in these species.

512 In general, we find that temperature is the strongest driver of repeated adaptation at both
513 the phenotypic and genomic levels. We quantified local adaptation at the phenotypic level using
514 correlations between traits measured in common gardens and the home environment of the
515 population they were sampled from. Across all phenotypes, these correlations tended to be
516 strongest and most similar among species for temperature variables, particularly in comparisons
517 among *H. annuus* and *H. petiolaris* subspecies (Figure S3). We see similar patterns of
518 repeatability reflected in the genome, where temperature variables also tend to have the greatest
519 repeatability (Figure 4). The similarity in these phenotypic and genomic signatures is consistent
520 with an effect of strong selection, as other artefactual or drift-based explanations for repeatability
521 would not be expected to reflect patterns found at the phenotypic level. It should be noted that
522 the reduced importance of soil variables in the SIPEC index might be partly driven by the fact
523 that all traits were measured on above-ground features, due to the difficulty of getting non-
524 disruptive phenotypic measurements for roots.

525 Taken together, these results suggest that some fraction of the genome contributes to
526 adaptation with low redundancy and high repeatability (which tends to be enriched within
527 genomic regions where there exist inversions in at least one species), while the remainder of the
528 adaptive response is driven by loci with high redundancy and species-specific contributions.
529 Theoretical models of adaptive evolution necessarily involve simplified representations of
530 genetics: population genetic approaches explore cases where strong selection deterministically
531 drives a change in allele frequency at one or a few loci (usually without epistasis), whereas
532 quantitative genetic approaches make the infinitesimal assumption that phenotypic change can be
533 realized through small frequency changes at many loci (Barton et al. 2017; Barghi et al. 2020;
534 Yeaman 2022). Such models implicitly make quite different assumptions about redundancy: if a
535 population genetic model of directional selection includes no epistasis then it is implicitly
536 assuming there is no redundancy, as every locus can increase fitness and no locus can affect the
537 potential of another locus to increase fitness. On the other hand, quantitative genetics models
538 implicitly assume complete redundancy, as the loci driving trait variation have interchangeable
539 effects. Given that differences in redundancy result in quite different evolutionary dynamics
540 (Höllinger et al 2019; Yeaman 2022), it is important to re-evaluate the behaviour of theoretical
541 models in light of what we can learn about redundancy from empirical data. Our results suggest
542 that adaptation is a complex process that does not map cleanly onto the assumptions of either
543 approach. At least some component of trait variation experiences sufficiently strong selection
544 and has low enough redundancy to drive the significant signatures of repeatability above the
545 random null that we observe here. On the other hand, most of the strongest signatures of
546 association are specific to a single species, implying high redundancy for most of the genome,
547 even if there are still some detectable signatures of repeatability. Such observations may be
548 consistent with classifying loci into "core" and "peripheral" sets similar to the omnigenic model,
549 but would involve classification based on redundancy rather than gene expression, as advocated
550 by Boyle et al. (2017). Theoretical models adopting a two-class representation of the genetic
551 basis of trait variation may provide more realism than models assuming a simpler distribution,
552 and perhaps yield new insights about qualitatively different dynamical behaviour. Given the
553 difficulty of rigourously quantifying the contribution of alleles of small effect and loci
554 contributing to local adaptation in only one species, it remains an open question what proportion
555 of adaptive response is governed by loci with dynamical behaviour that follow the infinitesimal

556 assumption. This could perhaps be quantified explicitly by decomposing heritabilities for traits
557 driving local adaptation, as has been done for standing variation in humans (Visscher et al.
558 2017), but this would require a considerable increase in sample size as methods such as GCTA
559 (Yang et al. 2011) do not yield accurate estimates at the sample sizes used here. Future work
560 could perhaps resolve this question using multi-generational crossing designs to break up the LD
561 that tends to accompany local adaptation, allowing a more accurate parsing of the effect sizes of
562 genomic regions and the contribution by repeated vs. redundant components of adaptive trait
563 variation.

564

565 **Materials and Methods**

566 **Data collection, common garden, and phenotyping.** Seed samples were collected from 151
567 wild sunflower populations covering most of their native distributions during the summer of
568 2015 (*H. annuus*: 61 populations for GWAS and 71 populations for GEA, *H. petiolaris fallax*: 23
569 populations, *H. petiolaris petiolaris:* 18 populations and *H. argophyllus*: 30 populations, Figure
570 1 and Supplementary Table 1). Seeds from ten additional populations of *H. annuus* for the GEA
571 analysis had been previously collected in the summer of 2011. Sample seeds were obtained from
572 randomly chosen mothers, and were first germinated in a greenhouse for two weeks, later moved
573 to an open-sided greenhouse for acclimation. Phenotypic data were collected throughout the
574 growing season, as detailed in Supplementary Table 1. Extensive records of developmental and
575 morphological traits throughout the growth of the plants including leaves, stem, and seeds which
576 were collected and digitally imaged to extract relevant phenotypic data.
577

578 **Similarity in Phenotype-Environment Correlation (SIPEC).** Locally adapted traits tend to
579 exhibit strong correlations between environment and common-garden phenotype. To estimate
580 which environmental variables are driving local adaptation for the same phenotype in pairs of
581 species, we calculate an index of the similarity in phenotype-environment correlation, SIPEC =
582 $(|r_1| + |r_2|)|r_1||r_2|$ where $r_1$ and $r_2$ are the Pearson correlations between the environment and
583 phenotype in the first and second species, respectively. This SIPEC index is maximized when the
584 correlation between a phenotype and an environmental variable is large in both species
585 regardless of the direction, so it does not differentiate phenotypically convergent vs. divergent

586 patterns of local adaptation (*e.g.*, increasing temperature causing an increase in flowering time in
587 one species and a decrease in the other), and provides a means of estimating the relative
588 importance of an environment driving local adaptation in both species in a similar way across all
589 measured phenotypes. To account for non-independence among traits, for each pair of species
590 we fit a PCA to all measured phenotypes and use the Principal Components that collectively
591 explain 95% of the variance, and calculate SIPEC on the correlations of each of these axes with
592 environment. For comparisons including *H. argophyllus*, 95% of the variance was typically
593 explained by 8-10 PC axes (out of 28 or 29 phenotypes), whereas for comparisons among other
594 taxa this included 21 or 22 PC axes (out of 65 or 66 phenotypes). We then report the maximum
595 and mean value of SIPEC for each environmental variable across these phenotypic PCA axes.

596

597 **Tests of SNP association with environment (GEA) and phenotype (GWAS).** A total of 39
598 environmental variables (21 climatic variables, 3 geographic variables, 15 soil variables
599 Supplementary Table 1) were used for the genotype-environment association analysis (GEA).
600 We refer to the climatic, soil and geographic variables collectively as the "environmental
601 variables", for simplicity. Soil data were collected by taking three to five soil samples collected
602 at each population from across the area in which seeds were collected and submitted to Midwest
603 Laboratories Inc. (Omaha, NE, USA) for analysis. Climate data for each population were
604 collected over a 30-year period (1961-1990) from geographic coordinates of the locations where
605 the samples were collected, using the software package Climate NA (Wang et al. 2012). We used
606 the package BAYPASS version 2.1 (Gautier 2015), which provides a re-implementation of the
607 Bayesian hierarchical model, and explicitly accounts for the covariance structure among the
608 population allele frequencies that originate from the shared history of the populations through the
609 estimation of the population covariance matrix. This renders the identification of SNPs subjected
610 to selection less sensitive to the confounding effect of population demography (Günther and
611 Coop 2013). Population structure was estimated by choosing a random and unlinked set of
612 10,000 SNPs and running BAYPASS under the core model (*i.e.*, no covariates). Then the Bayes
613 factors (BF) were calculated running BAYPASS under the STD covariate model to evaluate
614 association of SNPs with environmental variables (*i.e.*, adjusting for population structure). For
615 each SNP, the Bayes factor (denoted $BF_{is}$ as in Gautier 2015) was presented in decibian units

616 (db) via the transformation 10 $\log_{10}$ (BF). $BF_{is}$ relies on the importance sampling algorithm
617 proposed by Coop et al., 2010 and uses MCMC samples obtained under the core model. To
618 produce a narrower set of outlier loci, we followed the popular Jeffreys' rule (Jeffreys 1961) that
619 identified outlier loci with BF ≥ 10. As genome scan methods that correct for population
620 structure can remove some potential signals of local adaption when there is covariation between
621 the demographic history of the species and the environmental variables or phenotypic traits of
622 interest, we also calculated Spearman's rank correlation (ρ, uncorrected GEA) between
623 population allele frequencies for each SNP and each environment variable.
624 GWAS analysis was performed on 86, 30 and 69 developmental and morphologic traits in *H.*
625 *annuus, H. argophyllus* and *H. petiolaris,* respectively (Supplementary table 1). 29 variables
626 were measured in all three focal species, and 39 were measured only in *H. annuus* and in *H.*
627 *petiolaris* subspecies (Supplementary table 1). Seed and flower traits could not be collected for
628 *H. argophyllus*, since most plants of this species flowered very late in our common garden, and
629 failed to form fully developed inflorescences and set seeds before temperatures became too low
630 for their survival. Population structure was controlled for in GWAS by including the first three
631 principal components as covariates, as well as an identity-by-state (IBS) kinship matrix
632 calculated by EMMAX (Kang et al. 2010). We ran each trait GWAS using EMMAX
633 (v07Mar2010), as well as the EMMAX module in EasyGWAS (Grimm et al. 2017). For every
634 SNP/peak above the Bonferroni significance threshold, candidate genes were selected within a
635 100 Kb interval centered in the SNP with the lowest p-value, or within the boundaries of the
636 GWAS peak, whichever was larger. All variants used for association were initially filtered for
637 VQSR 90% tranche, and then further filtered to only include bi-allelic SNPs genotyped in ≥ 90%
638 of samples and with a minor allele frequency ≥ 3%.

639 **Identification of top-candidate windows.** We calculated the bottom 0.05 quantiles for the *p*-
640 values from association tests, Spearman's rank correlation (uncorrected GEA) and GWAS
641 (corrected and uncorrected), yielding two 5% cutoffs. For each environmental and phenotypic
642 variable, we identified all outlier SNPs as those that fell below the respective 5% cutoff. For
643 BayPass, we considered SNPs with Bayes factor ≥ 10 as outlier SNPs. For each 5 kb window
644 that we defined across the whole genome, we counted the number of outlier SNPs (*a*) and the
645 total number of SNPs (*n*). To identify top-candidate windows for each variable, we compared the

646 number of outlier SNPs per each 5 kb window to the 0.9999 quantile of the binomial expectation
647 where the expected frequency of outlier SNPs per window is calculated as: $\rho = \sum a_i/n_i$
648 (summation over all 5 kb windows), calculating $\rho$ independently for each environmental and
649 phenotype variable and excluding windows with 0 outliers from the calculation of $\rho$ (as per
650 Yeaman et al. 2016). We also calculated a top candidate index using the same approach to
651 categorize outliers, obtaining a *p*-value for a binomial test for the number of SNPs per window
652 given an expected proportion of outliers ($\rho$; this *p*-value is not exact due to non-independence of
653 SNPs so we refer to this as an index).

654 Identifying outlier SNPs detected by genome scans from genome-wide distribution without
655 accounting for local recombination rate variation can promote false positive signals in
656 recombination cold spots (*i.e.*, low recombination regions) and be overly conservative in
657 recombination hot spots (*i.e.*, high recombination regions) (Booker et al. 2020). Therefore, to
658 account for local recombination rate variation, all genomic windows were binned by their
659 estimated recombination rates into 5 equally sized bins (bin1: 0-20% quantile, bin2: 20%-40%
660 quantile, bin3: 40%-60% quantile, bin4: 60%-80% quantile, bin5: 80%-100% quantile). For each
661 recombination bin, we estimated expected frequency of SNPs per window ($\rho$) and calculated cut-
662 off separately. Windows falling above the threshold were identified as top candidate windows.

663 **Genome-wide survey of repeatability (null-W test).** To explore repeatable genomic signatures
664 of adaptation for each of the six pairwise contrasts among the 4 taxa (Figure 1), we used the
665 method developed by Yeaman et al. (2016) with some modifications. A common approach is to
666 identify candidates for adaptation independently in each species and then examine the overlap
667 between these lists, however this approach is quite stringent and may miss many interesting
668 signals. The null-W test is more sensitive, as it takes the list of top candidates from one species
669 and tests whether they tend to show more extreme signatures of association than expected by
670 chance. The null-W test is especially favorable when LD increased divergence of SNPs in tight
671 linkage with causal SNPs but did not raise the test values enough for a window to be classified as
672 an outlier according to the binomial test. For each top candidate window that we identified for
673 each focal species in a pair, we refer to the same window in the other species as "top candidate
674 ortholog". The null distribution for each focal species and variable was constructed by randomly
675 sampling 10,000 background SNPs from non-top candidate ortholog windows. For each non-top-

676 candidate window, we then estimated the test statistic (*W*) for the Wilcoxon-signed rank test vs.
677 the 10,000 background SNPs. This resulted in a null distribution representing the differences
678 between the 10,000 background SNPs and the non-top-candidate ortholog windows. These were
679 then standardized to *Z*-scores using the method in Whitlock and Schluter (2020):

680 $$Z = \frac{2W - n1n2}{\sqrt{n1n2(n1+n2+1)/3}} \qquad \text{(Equation 2)}$$

681

682 where n1 and n2 are the sample sizes being compared. In order to control for heterogeneity in
683 recombination rate and its possible effects on the null distribution, we estimated null distribution
684 for each recombination bin separately (5 in total, see above). We then compared the p-values and
685 bayes factors (BFs) for each focal top-candidate window to the 10,000 background SNPs,
686 calculating the W statistics and converting into a Z-score. Empirical P-values were then
687 calculated by comparing the Z-score for each top-candidate window to the null distribution.
688 When individual windows had values of W that exceeded the bounds of the null distribution,
689 their empirical *p*-value was set to the reciprocal of the number of genes in the null distribution.
690 For each species pair, we refer to the windows identified as significant by this test as "Windows
691 of Repeated Association" or WRAs.

692 **Linkage disequilibrium and detection of clusters of repeated association.** Linkage
693 disequilibrium among adjacent genomic windows can result in statistical non-independence and
694 similar GEA/GWAS signatures across many windows. To identify the most significant WRAs
695 and group neighbouring windows with similar signatures of repeatability into a single "Cluster of
696 Repeated Association" (CRA), we used the following approach in each pairwise contrast, and for
697 each environmental variable and phenotype: for each variable, empirical *p*-values for all WRAs
698 were converted to *q*-values to adjust for False Discovery, then beginning with the first significant
699 WRA along the chromosome (*i.e.*, with $q < 0.05$), we compared it to the next closest significant
700 WRA by calculating the squared Pearson correlation coefficient ($r^2$) on the allele frequencies
701 across all pairs of SNPs, and compared this estimate to a null distribution. To construct the null
702 distribution, we generated a distribution of LD measurements between 10,000 randomly chosen
703 windows with the same physical distance as between two significant WRAs (excluding all
704 WRAs from the null distribution). If the $r^2$ between the two neighboring significant WRAs was
705 greater than the 95$^{th}$ percentile of the null distribution, we clustered these two windows together.

706 This process was repeated successively with the next closest neighboring significant WRA,
707 walking out along the chromosome until one of two stopping criteria was reached: 1) the LD
708 between the last two windows did not exceed the 95 percent of the tail distribution or 2) the
709 distance between the initial window and the current window next to it was larger than 1 cM,
710 based on the linkage map from Todesco et al. (2020). When the first round of clustering stopped
711 due to either of these two criteria, all the clustered windows were removed from the dataset and
712 the process started with the second smallest empirical p-value. By doing this way, each
713 significant WRA will only appear in a single CRA.
714
715 **Estimating an index of shared standing variation.** As genotype calling was conducted
716 separately for each species (due to computational concerns), we estimated the amount of shared
717 standing variation based on counts of shared vs. non-shared SNPs. If two species are evolving
718 independently, the number of shared SNPs should follow a hypergeometric distribution, so we
719 used an approach similar to the C-scores (Yeaman et al. 2018) to calculate the difference
720 between the observed number of shared SNPs and the expectation, scaled by the standard
721 deviation of the hypergeometric. Because of noise and a relatively small number of SNPs per
722 window, we applied this approach on a sliding window basis, including the 5 flanking windows
723 upstream and downstream of each focal window the calculation of its index of shared standing
724 variation.

725 **Correspondence between regions of repeated association and chromosomal**
726 **rearrangements.** To assess the extent of overlap between regions of the genome with repeated
727 signatures of association and previously identified low-recombination haploblocks, we used two
728 approaches. Firstly, for each pairwise species contrast and variable, we constructed a
729 contingency table for the number of top candidates that were significant WRAs vs. not-
730 significant WRAs (by the null-W test), and that did vs. did not fall within a haploblock. We
731 calculated the Pearson's $\chi^2$ statistic on this table, and then permuted the location of haploblocks
732 throughout the genome to construct a null distribution of $\chi^2$ statistics, and calculated the p-value
733 as the proportion of the null that exceeded the observed $\chi^2$ statistic (to account for non-
734 independence of nearby WRAs), which is presented in Figure 5. Secondly, we compared
735 observations of the length and number of overlapping regions to expectations based on a

736 randomization approach. For each pair of species, we kept the position of each CRA constant
737 and randomized the position of haploblocks 10,000 times to build a null distribution. By keeping
738 the position of the CRAs constant, we maintained the architecture of adaptation independent
739 from chromosomal rearrangements. We assessed significance by testing whether the observed
740 overlaps between CRAs and haploblocks were more extreme than the 95$^{th}$ percentile of the tail of
741 null distribution, which is presented in Supplementary Figure S7. Details about identifying
742 chromosomal rearrangements can be found in Todesco et al. (2020).

743 **Identifying repeated signatures of association across all taxa**. As a complement to the
744 pairwise analysis, we used PicMin (Booker et al. 2022a) to identify windows of the genome with
745 strong signatures of association in multiple (sub-) species. For each environmental variable,
746 association signatures for each window are ranked genome-wide and PicMin identifies windows
747 with extreme ranks in multiple species. We ran the analysis once with each of the two 3-way
748 comparisons involving one *petiolaris* subspecies (*i.e.*, *H. annuus, H. argophyllus,* and either *H.*
749 *pet. petiolaris* or *H. pet. fallax*) to control for repeatability arising from similar patterns in the
750 two *petiolaris* subspecies (due to high introgression/shared standing variation).

751 **Evaluating genotypic redundancy using C-scores.** Genome-wide quantification of the
752 repeatability of association statistics provides insights into the amount of genotypic redundancy
753 underlying a trait or environmental adaptation, and can be assessed using the C-score approach
754 (Yeaman et al. 2018). Briefly, for a given trait or environment, the set of association test scores
755 within each species is classified into "associated" or "non-associated" using the binomial top
756 candidate approach. For a given pair of species ($i$ = 1, 2), the observed number of associated
757 windows in each species ($a_1$, $a_2$) can be compared to the number of windows that are associated
758 in both species ($a_b$) and the total number of windows being analysed ($a_x$). Under a null
759 hypothesis where all windows in the genome have equal potential to be involved in adaptation
760 (*i.e.*, associated with the trait or environment), the expected number of windows associated in
761 both species will be described by a hypergeometric distribution, with the expectation $\overline{a_b} =$
762 $a_1 a_2 / a_x$. The difference between the observed and expected amount of overlap in association
763 scores can be quantified as a C-score by scaling the difference by the standard deviation of the
764 hypergeometric (*i.e.*, a C-score of 2 means that the observed amount of overlap is two standard
765 deviations above the expectation under randomness).

766 We assess the C-scores for each phenotype and environment trait by classifying the top
767 0.5% of all 5 kb windows within each species as "associated" ($a_i$; based on the binomial top
768 candidate index), and begin by calculating the C-score obtained when $a_x$ is set to the union of $a_i$
769 across all four focal species/sub-species (*i.e.*, only those windows associated in at least one
770 species are included in $a_x$, a number much lower than the total number of windows in the
771 genome). This yields a negative C-score, as a random draw from such a small number of
772 windows tends to yield many more overlapping associations by chance than the observation.
773 When the C-score = 0, it means that the observed overlap between the pair of taxa being
774 considered is consistent with a random draw of their respective "associated" windows from an
775 overall pool of $a_x$ windows. Thus, by adding rows to the matrix with "non-associated" scores for
776 all 4 species/sub-species until finding the matrix that yields C-score = 0, we can estimate the
777 effective number of loci that contributed to variation for the trait or environment being
778 considered ($L_{eff}$), under the assumption that all such $a_x = L_{eff}$ windows had an equal chance of
779 contributing to the associations.
780 To run the C-score analysis on LD-clustered windows, we ran the following algorithm for
781 each trait/environmental variable: for each species, we identified all CRAs that also had a top
782 candidate index in top 0.5%. In most cases, a large cluster with associated windows in one
783 species corresponds to either no clusters or a small cluster in another species. To harmonize
784 cluster boundaries across species, we bin any overlapping clusters together to their maximum
785 extent, and take the average top candidate index for each cluster in each species as either: (a) the
786 mean across all windows that were "associated" in that species or (b) the average across all
787 windows associated in any species, if no windows were associated in that species. This yields a
788 matrix that can be submitted to the hypergeometric C-score analysis.

789

790 **Data availability**

791 All scripts used for analysis and figures are deposited in a Dryad archive at
792 doi:10.5061/dryad.wpzgmsbtd. Raw sequence data are deposited in the Sequence Read Archive
793 (SRA) under BioProject accessions PRJNA532579, PRJNA398560, and PRJNA564337, as
794 described in Todesco et al. (2020).

**Acknowledgements**:

The authors would like to thank the Yeaman and Peichel labs for comments. Computational support was provided by the Digital Resources Alliance of Canada, and funding was provided by Genome Canada and Genome BC (LSARP2014-223SUN), the International Consortium for Sunflower Genomic Resources, Alberta Innovates, and NSERC Discovery. GLO was funded by a Banting Postdoctoral Fellowship.

805 **References:**


806 Acharya BR, Raina S, Maqbool SB, Jagadeeswaran G, Mosher SL, Appel HM, Schultz JC,
807 Klessig DF, Raina R. 2007. Overexpression of CRK13, an Arabidopsis cysteine-rich
808 receptor-like kinase, results in enhanced resistance to Pseudomonas syringae:
809 Overexpression of CRK13 induces pathogen defense. *The Plant Journal* 50:488–499.

810 Auge GA, Penfield S, Donohue K. 2019. Pleiotropy in developmental regulation by flowering-
811 pathway genes: is it an evolutionary constraint? *New Phytol* 224:55–70.

812 Aukerman MJ, Sakai H. 2003. Regulation of Flowering Time and Floral Organ Identity by a
813 MicroRNA and Its *APETALA2* -Like Target Genes. *Plant Cell* 15:2730–2741.

814 Balasubramanian S, Sureshkumar S, Agrawal M, Michael TP, Wessinger C, Maloof JN, Clark R,
815 Warthmann N, Chory J, Weigel D. 2006. The PHYTOCHROME C photoreceptor gene
816 mediates natural variation in flowering and growth responses of Arabidopsis thaliana. *Nat*
817 *Genet* 38:711–715.

818 Barghi N, Hermisson J, Schlötterer C. 2020. Polygenic adaptation: a unifying framework to
819 understand positive selection. *Nat Rev Genet* 21:769–781.

820 Barton NH, Etheridge AM, Véber A. 2017. The infinitesimal model: Definition, derivation, and
821 implications. *Theoretical Population Biology* 118:50–73.

822 Bhatia N, Bozorg B, Larsson A, Ohno C, Jönsson H, Heisler MG. 2016. Auxin Acts through
823 MONOPTEROS to Regulate Plant Cell Polarity and Pattern Phyllotaxis. *Current Biology*
824 26:3202–3208.

825 Blackman BK, Scascitelli M, Kane NC, Luton HH, Rasmussen DA, Bye RA, Lentz DL,
826 Rieseberg LH. 2011. Sunflower domestication alleles support single domestication center
827 in eastern North America. *Proc. Natl. Acad. Sci. U.S.A.* 108:14360–14365.

828 Bohutínská M, Vlček J, Yair S, Laenen B, Konečná V, Fracassetti M, Slotte T, Kolář F. 2021.
829 Genomic basis of parallel adaptation varies with divergence in *Arabidopsis* and its
830 relatives. *Proc. Natl. Acad. Sci. U.S.A.* 118:e2022713118.

831 Booker TR, Yeaman S, Whitlock MC. 2020. Variation in recombination rate affects detection of
832 outliers in genome scans under neutrality. *Mol Ecol* 29:4274–4279.

833 Booker TR, Yeaman S, Whitlock MC. 2023a. Using genome scans to identify genes used
834 repeatedly for adaptation. *Evolution* 77:801-811.

835 Booker TR, Yeaman S, Whitlock MC. 2023b. The WZA: A window-based method for
836 characterizing genotype-environment association. *Mol Ecol Res* (in press).
837

838 Bürger R, Akerman A. 2011. The effects of linkage and gene flow on local adaptation: A two-
839 locus continent–island model. *Theoretical Population Biology* 80:272–288.

840 Chen A, Li C, Hu W, Lau MY, Lin H, Rockwell NC, Martin SS, Jernstedt JA, Lagarias JC,
841 Dubcovsky J. 2014. PHYTOCHROME C plays a major role in the acceleration of wheat
842 flowering under long-day photoperiod. *Proc. Natl. Acad. Sci. U.S.A.* 111:10037–10044.

843 Cheval C, Perez M, Leba LJ, Ranty B, Perochon A, Reichelt M, Mithöfer A, Robe E, Mazars C,
844 Galaud JP, et al. 2017. PRR2, a pseudo-response regulator, promotes salicylic acid and
845 camalexin accumulation during plant immunity. *Sci Rep* 7:6979.

846 Coughlan JM, Willis HJ. 2018. Dissecting the role of a large chromosomal inversion in life
847 history divergence throughout the Mimulus guttatus species complex. *Mol Ecol*. 28:1343-
848 1357.
849
850 DeRaad DA, Cobos ME, Alkishe A, Ashraf U, Ahadji-Dabla KM, Nuñez-Penichet C, Peterson
851 AT. 2021. Genome-environment association methods comparison supports omnigenic
852 adaptation to ecological niche in malaria vector mosquitoes. *Molecular Ecology* 30:6468–
853 6485.

854 Dong MA, Farré EM, Thomashow MF. 2011. CIRCADIAN CLOCK-ASSOCIATED 1 and
855 LATE ELONGATED HYPOCOTYL regulate expression of the C-REPEAT BINDING
856 FACTOR (CBF) pathway in *Arabidopsis*. *Proc. Natl. Acad. Sci. U.S.A.* 108:7241–7246.

857 Gautier M. 2015. Genome-Wide Scan for Adaptive Divergence and Association with
858 Population-Specific Covariates. *Genetics* 201:1555–1579.

859 Grimm DG, Roqueiro D, Salomé PA, Kleeberger S, Greshake B, Zhu W, Liu C, Lippert C,
860 Stegle O, Schölkopf B, et al. 2017. easyGWAS: A Cloud-Based Platform for Comparing
861 the Results of Genome-Wide Association Studies. *Plant Cell* 29:5–19.

862 Günther T, Coop G. 2013. Robust Identification of Local Adaptation from Allele Frequencies.
863 *Genetics* 195:205–220.

864 Hager ER, Harringmeyer OS, Wooldridge TB, Theingi S, Gable JT, McFadden S, Neugeboren
865 B, Turner KM, Jensen JD, Hoekstra HE. 2022. A chromosomal inversion contributes to
866 divergence in multiple traits between deer mouse ecotypes. *Science* 377:399–405.

867 Heiser C, Smith D, Clevenger S, Martin W. 1969. The North American sunflowers (Helianthus).
868 *Memoirs of the Torrey Botanical Club* 22:1–218.

869 Heiser, CB. 1951. Hybridization in the Annual Sunflowers: Helianthus annuus x H. argophyllus.
870 *The American Naturalist* 85:65–72.

871 Hoban S, Kelley JL, Lotterhos KE, Antolin MF, Bradburd G, Lowry DB, Poss ML, Reed LK,
872 Storfer A, Whitlock MC. 2016. Finding the Genomic Basis of Local Adaptation: Pitfalls,
873 Practical Solutions, and Future Directions. *The American Naturalist* 188:379–397.

874 Höllinger I, Pennings PS, Hermisson J. 2019. Polygenic adaptation: from sweeps to subtle
875 frequency shifts. PLoS Genet. 15:e1008035.
876

Izawa T. 2007. Adaptation of flowering-time by natural and artificial selection in Arabidopsis and rice. *Journal of Experimental Botany* 58:3091–3097.

Jeffreys H. 1961. Theory of probability. 3rd ed. New York, NY: Oxford University Press

Kang HM, Sul JH, Service SK, Zaitlen NA, Kong S, Freimer NB, Sabatti C, Eskin E. 2010. Variance component model to account for sample structure in genome-wide association studies. *Nat Genet* 42:348–354.

Keuskamp DH, Pollmann S, Voesenek LACJ, Peeters AJM, Pierik R. 2010. Auxin transport through PIN-FORMED 3 (PIN3) controls shade avoidance and fitness during competition. *Proc. Natl. Acad. Sci. U.S.A.* 107:22740–22744.

Kirkpatrick M, Barton N. 2006. Chromosome Inversions, Local Adaptation and Speciation. *Genetics* 173:419–434.

Láruson ÁJ, Yeaman S, Lotterhos KE. 2020. The Importance of Genetic Redundancy in Evolution. *Trends in Ecology & Evolution* 35:809–822.

Lee C-R, Wang B, Mojica JP, Mandáková T, Prasad KVSK, Goicoechea JL, Perera N, Hellsten U, Hundley HN, Johnson J, et al. 2017. Young inversion with multiple linked QTLs under selection in a hybrid zone. *Nat Ecol Evol* 1:0119.

Liu Z, Jia Y, Ding Y, Shi Y, Li Z, Guo Y, Gong Z, Yang S. 2017. Plasma Membrane CRPK1-Mediated Phosphorylation of 14-3-3 Proteins Induces Their Nuclear Import to Fine-Tune CBF Signaling during Cold Response. *Molecular Cell* 66:117-128.e5.

Lotterhos KE, Whitlock MC. 2014. Evaluation of demographic history and neutral parameterization on the performance of $F_{ST}$ outlier tests. *Mol Ecol* 23:2178–2192.

MacPherson A, Nuismer SL. 2017. The probability of parallel genetic evolution from standing genetic variation. *J. Evol. Biol.* 30:326–337.

Manceau M, Domingues VS, Linnen CR, Rosenblum EB, Hoekstra HE. 2010. Convergence in pigmentation at multiple levels: mutations, genes and function. *Phil. Trans. R. Soc. B* 365:2439–2450.

Mizoguchi T, Wheatley K, Hanzawa Y, Wright L, Mizoguchi M, Song HR, Carré IA, Coupland G. 2002. LHY and CCA1 are partially redundant genes required to maintain circadian rhythms in Arabidopsis. *Dev Cell* 2:629–641.

Moyers BT, Rieseberg LH. 2016. Remarkable life history polymorphism may be evolving under divergent selection in the silverleaf sunflower. *Mol Ecol* 25:3817–3830.

Ostevik KL, Andrew RL, Otto SP, Rieseberg LH. 2016. Multiple reproductive barriers separate recently diverged sunflower ecotypes: reproductive barriers between sunflower ecotypes. *Evolution* 70:2322–2335.

912 Para A, Farré EM, Imaizumi T, Pruneda-Paz JL, Harmon FG, Kay SA. 2007. PRR3 Is a vascular
913 regulator of TOC1 stability in the Arabidopsis circadian clock. *Plant Cell* 19:3462–3473.

914 Pekker I, Alvarez JP, Eshed Y. 2005. Auxin response factors mediate Arabidopsis organ
915 asymmetry via modulation of KANADI activity. *Plant Cell* 17:2899–2910.

916 Rosenblum EB, Parent CE, Brandt EE. 2014. The Molecular Basis of Phenotypic Convergence.
917 *Annu. Rev. Ecol. Evol. Syst.* 45:203–226.

918 Sambatti JBM, Strasburg JL, Ortiz-Barrientos D, Baack EJ, Rieseberg LH. 2012. Reconciling
919 extremely strong barriers with high levels of gene exchange in annual sunflowers: gene
920 flow across a strong reproductive barrier. *Evolution* 66:1459–1473.

921 Schaal SM, Haller BC, Lotterhos KE. 2022. Inversion invasions: when the genetic basis of local
922 adaptation is concentrated within inversions in the face of gene flow. *Phil. Trans. R. Soc.*
923 *B* 377:20210200.

924 Strasburg JL, Rieseberg LH. 2008. Molecular demographic history of the annual sunflowers
925 *helianthus annuus* and *h. Petiolaris* -large effective population sizes and rates of long-
926 term gene flow. *Evolution* 62:1936–1950.

927 Takano M, Inagaki N, Xie X, Yuzurihara N, Hihara F, Ishizuka T, Yano M, Nishimura M,
928 Miyao A, Hirochika H, et al. 2005. Distinct and Cooperative Functions of Phytochromes
929 A, B, and C in the Control of Deetiolation and Flowering in Rice. *The Plant Cell*
930 17:3311–3325.

931 Tittes S, Lorant A, McGinty S, Doebley JF, Holland JB, Sánchez-González J de J, Seetharam A,
932 Tenaillon M, Ross-Ibarra J. 2021. Not so local: the population genetics of convergent
933 adaptation in maize and teosinte. Evolutionary Biology Available from:
934 http://biorxiv.org/lookup/doi/10.1101/2021.09.09.459637

935 Todesco M, Owens GL, Bercovich N, Légaré J-S, Soudi S, Burge DO, Huang K, Ostevik KL,
936 Drummond EBM, Imerovski I, et al. 2020. Massive haplotypes underlie ecotypic
937 differentiation in sunflowers. *Nature* 584:602–607.

938 Visscher PM, Wray NR, Zhang Q, Sklar P, McCarthy MI, Brown MA, Yang J. 2017. 10 Years
939 of GWAS Discovery: Biology, Function, and Translation. *The American Journal of*
940 *Human Genetics* 101:5–22.

941 Wang L, Josephs EB, Lee KM, Roberts LM, Rellán-Álvarez R, Ross-Ibarra J, Hufford MB.
942 2021. Molecular Parallelism Underlies Convergent Highland Adaptation of Maize
943 Landraces.Purugganan M, editor. *Molecular Biology and Evolution* 38:3567–3580.

944 Wang T, Hamann A, Spittlehouse DL, Murdock TQ. 2012. ClimateWNA—High-Resolution
945 Spatial Climate Data for Western North America. *Journal Of Applied Meteorology And*
946 *Climatology* 51:14.

947 Wellenreuther M, Bernatchez L. 2018. Eco-Evolutionary Genomics of Chromosomal Inversions.
948 *Trends in Ecology & Evolution* 33:427–440.

949 Whitlock M, Schluter D. 2020. The analysis of biological data. 3rd ed. Macmillan

950 Yang J, Lee SH, Goddard ME, Visscher PM. 2011. GCTA: A Tool for Genome-wide Complex
951 Trait Analysis. *The American Journal of Human Genetics* 88:76–82.

952 Yeaman S. 2022. Evolution of polygenic traits under global *vs* local adaptation. *Genetics*
953 220:iyab134.

954 Yeaman S, Gerstein AC, Hodgins KA, Whitlock MC. 2018. Quantifying how constraints limit
955 the diversity of viable routes to adaptation.Ralph PL, editor. *PLoS Genet* 14:e1007717.

956 Yeaman S, Hodgins KA, Lotterhos KE, Suren H, Nadeau S, Degner JC, Nurkowski KA, Smets
957 P, Wang T, Gray LK, et al. 2016. Convergent local adaptation to climate in distantly
958 related conifers. *Science* 353:1431–1433.

959 Yeaman S, Whitlock MC. 2011. The genetic architecture of adaptation under migration-selection
960 balance: the genetic architecture of local adaptation. *Evolution* 65:1897–1911.

961

962

963

964